2019 SECED Conference
Earthquake risk and engineering towards a resilient world
9-10 September 2019, Greenwich, London

THE RESPONSE OF PLATES UNDER NON-UNIFORM IMPULSIVE LOADS

Sam RIGBY[1]*, Andy TYAS[1], Richard CURRY[2], Genevieve LANGDON[2]

Abstract: *Near-field blast loads are non-uniformly distributed across the loaded face of a structural element and result in large, localised plastic deformations. Experimental characterisation of both the loading and resultant deformation is rare in the literature, and to date there have been no studies which investigate modes and mechanisms of target deformation with a detailed knowledge of the imparted load. This paper presents results from a collaboration between the University of Sheffield, UK, and the University of Cape Town, South Africa, aimed at measuring the loading imparted to, and subsequent dynamic deformation of blast loaded plates. This paper presents results from these experiments, where the presence of inward and outward travelling flexural waves are observed and discussed in relation to localised variations in the imparted load.*

Introduction

Blast protection engineering aims to provide effective and efficient systems to resist against blast loads. Accordingly, it is necessary to understand both the form, magnitude, and distribution of the load imparted from a given blast event, *and* the subsequent response of a structural system subjected to this load. The blast load from a near-field explosion (within approximately 10-20 radii of a spherical explosive) is characterised by a near-instantaneous rise to peak pressures in the order of 100-1,000 MPa, followed by a rapid decay to ambient conditions typically occurring within sub-ms of arrival of the blast wave. Subsequent structural response reaches a peak value in the order of 10-100 mm and, whilst structural response periods tend to be orders of magnitude slower than load application, deformation cycles are still within ms durations. Clearly, accurate experimental quantification of these two quantities (loading and deformation) presents a significant challenge to the research community.

The University of Sheffield (UoS), UK, and the University of Cape Town (UCT), South Africa, have established track records in experimental quantification of blast loading (Clarke et al 2015) and dynamic target deformation (Curry and Langdon 2017). In this paper, we present a combined experimental study where similar scaled tests are performed at UoS and UCT and are used to jointly interrogate the performance of blast loaded plates. In particular, two different explosive configurations are used in which each produces a different level of loading symmetry/regularity, and the influence of these irregularities on target deformation is discussed.

Experimental work

The *Characterisation of Blast Loading* apparatus (Rigby et al 2014, Clarke et al 2015) at the UoS Blast & Impact Laboratory comprises a nominally target plate, mounted to a stiff, massive reinforced concrete frame. Hopkinson (1914) pressure bars (HPBs) are inserted through the target plate and sit flush with its surface, such that blast pressures acting on the target plate, arising from detonation of a high explosive located a short distance from the face of the plate, act concurrently on the faces of the HPBs. In the current arrangement, 17 HPBs are located within a 200 mm diameter region of the target plate: one bar directly in line with the charge centre, and four bars each at 25, 50, 75, and 100 mm from the central bar. Axial strains are recorded on the perimeters of the HPBs and are used to determine the spatial and temporal distribution of pressure on the loaded face. This apparatus has been used previously to record blast pressures at scaled distances between 0.1-1.0 m/kg$^{1/3}$ (Tyas et al 2016).

[1] Department of Civil & Structural Engineering, University of Sheffield, UK
[2] Blast Impact and Survivability Research Unit, Department of Mechanical Engineering, University of Cape Town, South Africa
* sam.rigby@sheffield.ac.uk

The *DIC Blast Pendulum* at the Blast Impact and Survivability Research Unit (BISRU) UCT comprises a cable-suspended I-beam with a clamping frame at the front (to house the target plates) and a laser displacement gauge aimed at the rear of the pendulum to measure its motion, thus allowing total imparted impulse to be calculated. The apparatus was recently modified (see Curry and Langdon 2017 for more information) to house two stereo high speed video (HSV) cameras which are used to record motion of the rear face of the target plates. Digital image correlation (DIC) is used to calculate transient out-of-plane displacement profiles of the test plates. More detail is available in Rigby et al (2019a, 2019b).

In this study, the test plates were made from 400×400×3 mm thick Domex 355MC steel (7830 kg/m^3) with an exposed circular area of 300 mm diameter when loaded in the clamping frame. The plates were fully clamped around the perimeter, with imposed constraints of zero in-plane and out-of-plane displacement and zero rotations at the boundary.

Tests at UCT were limited to 50 g PE4, so Hopkinson-Cranz scaling (Hopkinson 1915, Cranz 1926) is used to compare between UoS and UCT scales. Accordingly, distances, times and specific impulses are scaled by the relative cube-root of the charge masses, thus:

$$\frac{x_{UoS}}{x_{UCT}} = \frac{i_{UoS}}{i_{UCT}} = \sqrt[3]{\frac{W_{UoS}}{W_{UCT}}} \tag{1}$$

where x, i, and W are distance from the centre of the plate, specific impulse, and charge mass, and the subscripts UoS and UCT refer to quantities used in the University of Sheffield and University of Cape Town tests respectively.

Six tests were performed at UoS: three tests using 100 g spherical PE4 charges, centrally detonated, located at 55.4 mm clear stand-off distance from the centre of the rigid target; and three tests using 78 g cylindrical PE4 charges (3:1 diameter:height ratio) located at 168.0 mm clear stand-off distance from the centre of the rigid target. In this article, these tests are referred to as UoS Sph T1-3 and UoS Cyl T1-3 respectively.

Ten tests were performed at UCT and were designed to match the scaled geometries of the UoS tests: three tests using 50 g spherical PE4 charges, centrally detonated, located at 44.0 mm clear stand-off distance from the centre of the target plates; and three tests using 50 g cylindrical PE4 charges (3:1 d:h) located at 145.0 mm clear stand-off distance from the centre of the target plates. In this article, these tests are referred to as UCT Sph T1-5 and UCT Cyl T1-5 respectively. In the UCT experiments, the first two tests for each charge configuration were performed without DIC and hence peak dynamic deflections are unavailable for these tests. Residual plate deformation, however, was recorded in all UCT tests. The test programme is summarised in Table 1.

Test number	Charge mass (g PE4)	Clear stand-off (mm)	Charge radius (mm)	Charge shape	Diagnostics
UoS Sph T1-3	100	55.4	24.6	Sphere	HPBs
UoS Cyl T1-3	78	168.0	28.6	3:1 (d:h) cylinder	HPBs
UCT Sph T1-2	50	44.0	19.5	Sphere	Impulse only
UCT Sph T3-5	50	44.0	19.5	Sphere	Impulse and DIC
UCT Cyl T1-2	50	145.0	24.5	3:1 (d:h) cylinder	Impulse only
UCT Cyl T3-5	50	145.0	24.5	3:1 (d:h) cylinder	Impulse and DIC

Table 1. Summary of experimental work

Localised variations in specific impulse distribution

Specific impulse distributions for UoS Sph T1-3 and UoS Cyl T1-3 are shown in Figure 1. Here, individual target markers represent the recorded data (separated by test) and the solid lines show a cubic spline interpolant fitted to the mean values of all recorded data at each bar location (symmetric in positive and negative radial ordinates). It has been shown that numerical modelling results closely match this mean distribution (Rigby, Fuller and Tyas 2018). In Figure 1, major axes show as-recorded magnitudes, and minor axes (light grey) show these values expressed at UCT scale (50g PE4). The total area integrated impulse of the mean distribution (I), is shown for both scales.

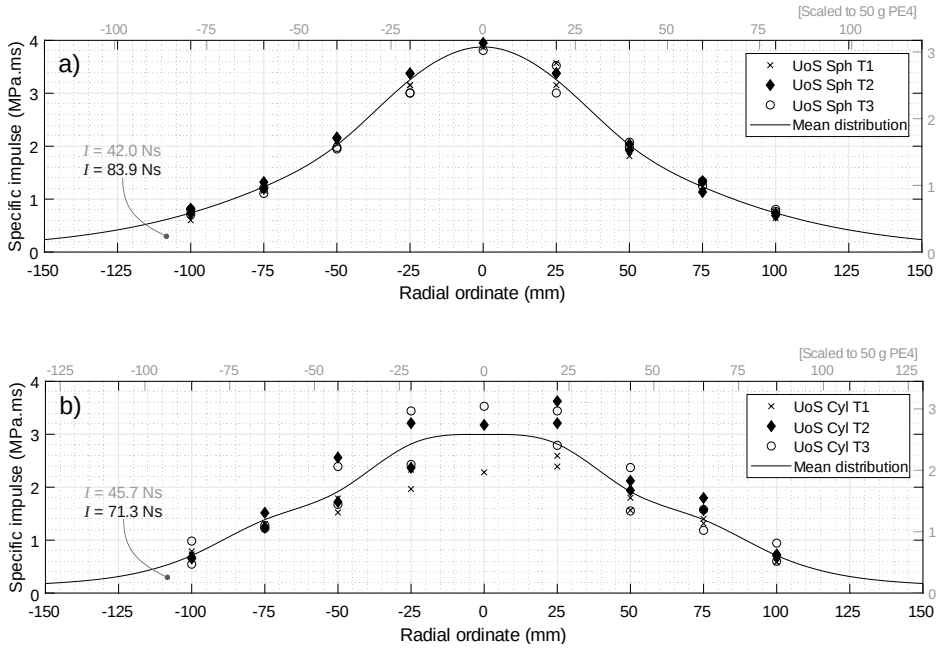

Figure 1. Peak specific impulse and mean distributions for spherical (a) and cylindrical (b) tests respectively. Results are expressed at UCT scale (50 g PE4) on minor axes

It is clear that the spherical specific impulses occupy a tight banding around the mean distribution, and therefore in any given test the load is likely to be highly symmetrical and regular. Conversely, the cylindrical data occupies a wider band either side of the mean, and whilst the mean distribution is similar to the mean distribution from the spherical tests, the loading distribution *for a given test* is likely to be unsymmetrical with highly localised variations in specific impulse. Take, for example, the specific impulse at 25 mm from the centre of the plate for UoS Cyl T2. Here, the maximum recorded specific impulse was 3.63 MPa.ms and the minimum was 2.37 MPa.ms, a deviation of +/-30% from the mean within less than one charge radii from the centre of the target. The specific impulse recorded at 25 mm from the centre was the largest recorded specific impulse for this test.

It is hypothesised that these irregularities in the loading are caused by the growth of Rayleigh-Taylor and Richtmyer-Meshkov instabilities (Tyas et al 2016). In the spherical tests, the target is located approximately 2 charge radii from the explosive, whereas in the cylindrical tests the target is approximately 6 radii from the explosive. An increased distance is likely to enhance the development of these instabilities. To illustrate this, Figure 2 shows approximate outlines of the detonation product cloud (DPC) from UoS Cyl T1 and T2, determined from post-processing each frame of HSV data recorded (at 140,000 fps) as part of these experiments. It is clear that the interface between the explosive and DPC is highly variable and non-symmetric, particularly in the later frames immediately before it impinges on the target plate (at y=177.5 mm). A critical aspect of this study is investigating the influence that these localised variations have on the deformation of blast loaded targets. Note: HSV stills from the spherical charge tests did not exhibit any significant deviation in shape of the DPC prior to impingement on the target plate.

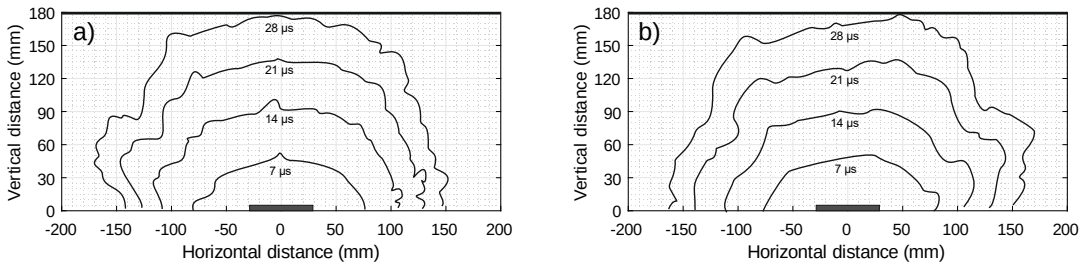

Figure 2. Outlines of the detonation product cloud from post-processing of high speed video stills from UoS Cyl T1 (a) and UoS Cyl T2 (b)

Total impulse recorded in UCT tests and agreement with UoS tests

Table 2 shows the measured total impulse from the UCT tests, compared against the UoS area-integrated impulse given by the mean distributions for the spherical and cylindrical charges (expressed at UCT scale in the 'factored impulse' column using Hopkinson-Cranz scaling). Here, the UCT impulses have been factored by 0.67 after the numerical analyses of Bonorchis and Nuick (2009) showed that, for this apparatus, the impulse acting on the target plate is approximately 67% of the total impulse recorded by the pendulum.

It can be seen that the two different measurement techniques (integration of HPB signals and the pendulum) recorded impulses that are in close agreement, and there is relatively little deviation from test-to-test (all values within 6% of the mean) when considering total, area-integrated impulse.

Test number	Measured impulse (Ns)	Factored impulse (Ns)	Deviation from UCT mean	Deviation from UoS mean
UCT Sph T1	65.5	43.9*	-0.7 %	+4.5 %
UCT Sph T2	68.3	45.8*	+3.6 %	+9.0 %
UCT Sph T3	65.8	44.1*	-0.2 %	+5.0 %
UCT Sph T4	66.1	44.3*	+0.2 %	+5.5 %
UCT Sph T5	64.3	43.1*	-2.5 %	+2.6 %
Mean, UCT Sph T1-5	**66.0**	**44.2***	**n/a**	**+5.2 %**
Mean, UoS Sph T1-3	**83.9**	**42.0†**	**-5.0 %**	**n/a**
UCT Cyl T1	71.1	47.6*	+5.8 %	+4.2 %
UCT Cyl T2	65.4	43.8*	-2.7 %	-4.2 %
UCT Cyl T3	67.0	44.9*	-0.2 %	-1.8 %
UCT Cyl T4	68.8	46.1*	+2.4 %	+0.9 %
UCT Cyl T5	63.4	42.5*	-5.6 %	-7.0 %
Mean, UCT Cyl T1-5	**67.1**	**45.0***	**n/a**	**-1.5 %**
Mean, UoS Cyl T1-3	**71.3**	**45.7‡**	**+1.6 %**	**n/a**

Table 2. Summary of measured total impulses from UCT and UoS tests.

Influence of localised loading variations on plate deformation

Whilst the irregularities detected in the UoS tests seem to have little significance on the total impulse imparted to the plates (i.e. low test-to-test variation), it is interesting to determine whether these features influence structural displacement: i.e. do deformations in the cylindrical charge tests exhibit higher test-to-test variations and asymmetries when compared to the spherical charge tests?

Table 3 shows residual deflection (determined from post-test laser scans of the plates) and peak dynamic deflection (determined from DIC data) recorded in the UCT tests, alongside their corresponding deviations from the mean value for each charge configuration. It is interesting to note that, whilst the spherical charge tests exhibit a low test-to-test variability (all tests within 4% of the mean for both residual and dynamic deflection), the cylindrical charge tests exhibit a much higher test-to-test variability, with the residual and dynamic deflections for UCT Cyl T3 approximately 14% lower than the mean values. Whilst this may seem anomalous, it is worth noting that this increased variability in deformation for the cylindrical charge tests is in agreement with the findings from the specific impulse data recorded in the UoS tests. This suggests that localised variations in loading, caused by Rayleigh-Taylor and Richtmyer-Meshkov instabilities, appear to affect the transient and residual displacement of a blast loaded target.

* denotes impulse acting on the exposed area has been estimated by factoring the total impulse by 0.67, after Bonorchis and Nuick (2009)

† denotes UoS tests have been scaled by 50/100 = 0.50 to express the results at UCT scale, according to Hopkinson-Cranz scaling (Hopkinson 1915, Cranz 1926)

‡ denotes UoS tests have been scaled by 50/78 = 0.64 to express the results at UCT scale, according to Hopkinson-Cranz scaling (Hopkinson 1915, Cranz 1926)

Test number	Residual deflection (mm)	Deviation from mean	Dynamic deflection (mm)	Deviation from mean
UCT Sph T1	15.39	-3.0 %	–	–
UCT Sph T2	16.31	+2.8 %	–	–
UCT Sph T3	15.81	-0.3 %	21.27	+3.6 %
UCT Sph T4	15.82	-0.3 %	19.95	-2.9 %
UCT Sph T5	15.96	+0.6 %	20.40	-0.7 %
Mean, UCT Sph T1-5	**15.86**	**n/a**	**20.54**	**n/a**
UCT Cyl T1	18.77	+4.8 %	–	–
UCT Cyl T2	19.17	+7.0 %	–	–
UCT Cyl T3	15.29	-14.6 %	19.01	-13.4 %
UCT Cyl T4	18.17	+1.5 %	23.48	+6.9 %
UCT Cyl T5	18.15	+1.3 %	23.38	+6.5 %
Mean, UCT Cyl T1-5	**17.91**	**n/a**	**21.96**	**n/a**

Table 3. Summary of residual and dynamic deflection results from UCT tests.

To further investigate this, DIC data were post-processed in order to determine plate velocity profiles (Rigby et al 2017) and highlight the existence of flexural waves in the plate. In Figure 3(a), DIC data from UCT Sph T3 is plotted as an out-of-plane displacement vs distance vs time filled contour plot, where 0 and 300 mm on the vertical axis represent the edges of the plate, and 150 mm represents the plate centre. There appear to be two displacement peaks, one at 0.4 ms after detonation, and one at 0.7 ms. Figure 3(b) shows the out-of-plane velocity profile of the plate for the same test, determined from linear central differencing of the displacement data. Close inspection of the velocity profile reveals the existence of flexural waves.

There appear to be two sets of flexural waves: one set beginning in the centre of the plate and propagating outwards towards the supports, and one set beginning at the supports and travelling inwards towards the plate centre. This behaviour is consistent with wave propagation associated with concentrated and uniform loads respectively, and is indicative of the shape of the load curve in Figure 1(a), i.e. a load that is highly concentrated in the centre and relatively uniform at the periphery of the target. The approximate location of these waves is indicated in Figure 3(c), according to the author's best judgement. The displacement peaks at 0.4 and 0.7 ms appear to coincide with the crossing of the inward and outward travelling flexural waves at the plate centre respectively.

Figure 4(a) shows out-of-plane displacement vs distance vs time for UCT Cyl T3, and Figure 4(b) shows out-of-plane velocity vs distance vs time. Again, flexural wave locations (from processing of the velocity data) are shown in Figure 4(c). Whilst the magnitudes of displacement and velocity are broadly similar to those from Figure 3, there are significant differences when the flexural wave behaviour is compared to the spherical charge test. These can be summarised in two key observations.

Firstly, it appears as though peak velocities are developed at some distance away from the centre of the plate (at an approximate distance of 130 mm, i.e. 20 mm off-centre). This results in unsymmetrical propagation of the pair of outward travelling flexural waves, which arrive at the plate edge some 50 µs apart and cross at 0.72 ms, approximately 20 mm off-centre on the opposite side of the plate centre to where the impact point was judged to have occurred. Displacement data from Figure 3(a) suggested that these flexural waves were in part responsible for slight increases in plate displacement when they crossed at the plate centre. That these waves in UCT Cyl T3 were seen to cross off-centre may partly explain (in addition to the original non-central impingement of the blast wave) why dynamic and residual displacements were lower for this test (Table 3), despite the total recorded impulse closely matching the mean for the cylindrical charge tests (Table 2).

Secondly, there is a low magnitude flexural wave in Figure 4(c), which appears to be generated at the point (0.02 ms, 220 mm). This is significant as it suggests that some component of the load has been imparted *before* the arrival of the main shock front, significantly off-centre.

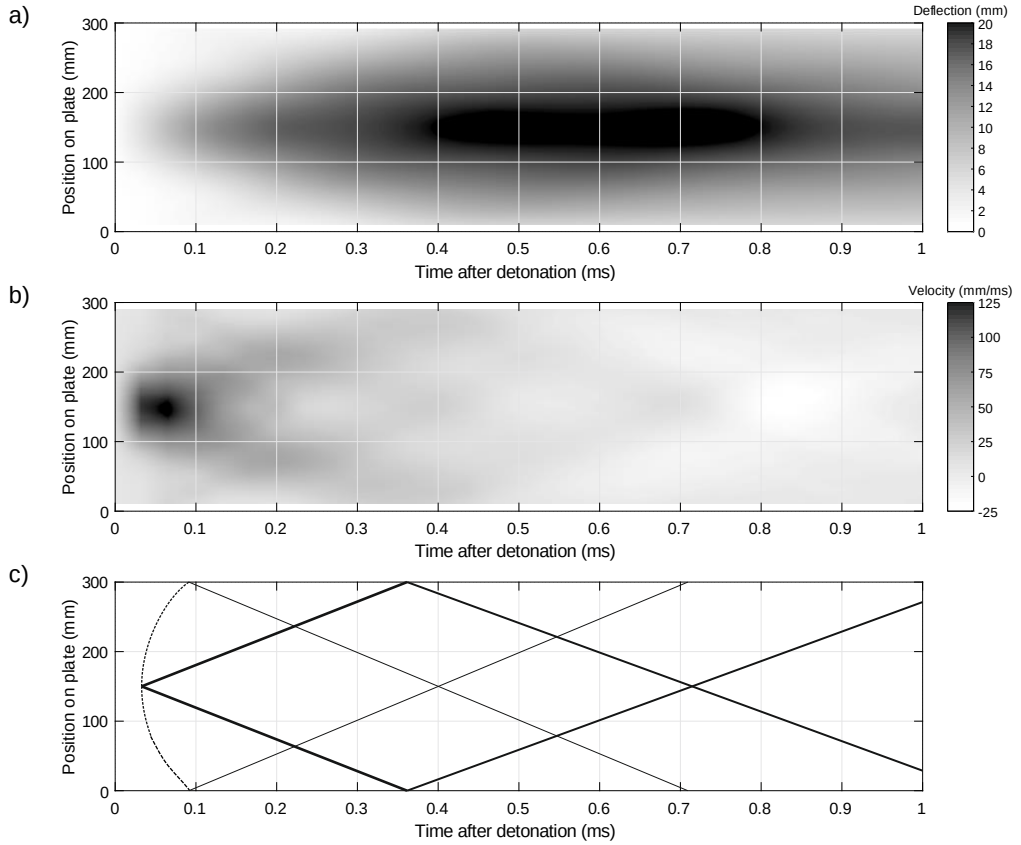

Figure 3. Out-of-plane displacement vs distance vs time (a) and out-of-plane velocity vs distance vs time (b) from UCT Sph T3, with approximate location of flexural waves indicated (c)

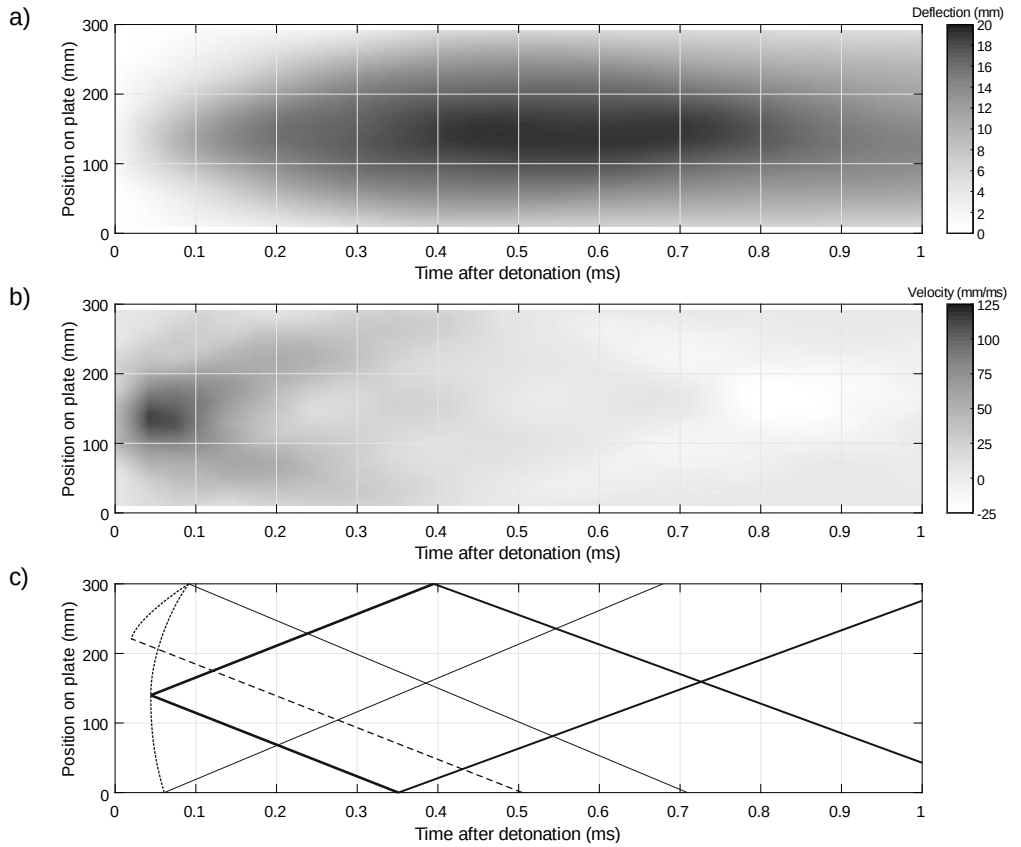

Figure 4. Out-of-plane displacement vs distance vs time (a) and out-of-plane velocity vs distance vs time (b) from UCT Cyl T3, with approximate location of flexural waves indicated (c)

This appears to support observations from the UoS tests, in particular UoS Cyl T2 where the peak recorded specific impulse was 25 mm from the centre of the plate (22 mm at UCT scale, see Figure 1(b)). The DPC in this test also appeared to strike the target first at ~50 mm from the centre of the plate (see Figure 2(b)). It is evident, therefore, that localised variations in the shape, velocity, and pressure of the DPC can have a significant influence on the subsequent displacement of a blast loaded plate.

Summary and conclusions

This paper presents experimental results from a collaborative study between the University of Sheffield and the University of Cape Town. Here, loading distributions and dynamic target deformations were measured in separate trials using spherical and cylindrical explosive charges. The cylindrical charges were shown to demonstrate higher localised variabilities in the loading, caused by the growth of Rayleigh-Taylor and Richtmyer-Meshkov instabilities, whereas the spherical charges were shown to produce a highly repeatable and symmetric loading distribution.

Plate deformations in the cylindrical charge tests were also more variable than those from the spherical charge tests. Digital image correlation data were examined and used to highlight the presence of flexural waves in the plates. Again, these flexural waves were seen to be regular and repeatable in the spherical charge tests, but were less so in the cylindrical charge tests. The results presented herein suggest that localised variations in a blast load can be significant to influence the dynamic displacement of a blast loaded plate. This research has particular application for thin-shelled structures, where local differences in deformation velocity may be significant to cause differential shear failure. Research is ongoing on this topic.

References

Bonorchis D and Nurick GN (2009), The influence of boundary conditions on the loading of rectangular plates subjected to localised blast loading – importance in numerical simulations. *International Journal of Impact Engineering*, **36**(1):40–52

Clarke SD et al. (2015), A large scale experimental approach to the measurement of spatially and temporally localised loading from the detonation of shallow-buried explosives. *Measurement Science and Technology*, **26**:015001

Cranz C (1926), *Lehrbuch der Basllistik*. Springer, Berlin, Germany

Curry RJ and Langdon GS (2017), Transient response of steel plates subjected to close proximity explosive detonations in air. *International Journal of Impact Engineering*, **102**:102–116

Hopkinson B (1914), A method of measuring the pressure produced in the detonation of high explosives or by the impact of bullets. *Philosophical Transactions of the Royal Society of London. Series A, Containing Papers of a Mathematical or Physical Character*, **213**(1914):437–456

Hopkinson B (1915), *British Ordnance Board Minutes*, Report 13565, British Ordnance Office, London, UK

Rigby SE et al. (2014), Testing apparatus for the spatial and temporal pressure measurements from near-field free air explosions. In: *Proceedings of the 6th International Conference on Protection of Structures Against Hazards (PSH14)*, Tianjin, China

Rigby SE, Curry RJ, Langdon GS and Tyas A (2017), Initial velocity and impulse distribution of blast loaded plates. *In: Proceedings of the 17th International Symposium on Interaction of the Effects of Munitions with Structures (ISIEMS17)*, Bad Neuenahr, Germany

Rigby, SE, Fuller BJ and Tyas A (2018), Validation of near-field blast loading in LS-DYNA. In: *Proceedings of the 5th International Conference on Protective Structures (ICPS5)*, Poznan, Poland.

Rigby SE, Tyas A, Curry RJ, and Langdon GS (2019a), Experimental measurement of specific impulse distribution and transient deformation of plates subjected to near-field explosive blasts. *Experimental Mechanics*, **59**(2), 163–178

Rigby SE et al. (2019b), Predicting the response of plates subjected to near-field explosions using an energy equivalent impulse. *International Journal of Impact Engineering*, **128**, 24–36

Tyas A et al. (2016), Experimental studies of the effect of rapid afterburn on shock development of near-field explosions. *International Journal of Protective Structures*, **7**(3), 456–465